The 3rd International Conference on Structural Health Monitoring of Intelligent Infrastructure
Vancouver, British Columbia, Canada
November 13-16, 2007

SMART MAGNETORHEOLOGICAL DAMPERS WITH EMBEDDED SENSORS FOR VIBRATION CONTROL APPLICATIONS

K. H. Lam
The Hong Kong Polytechnic University, China

Z. H. Chen
The Hong Kong Polytechnic University, China

S. W. Or
The Hong Kong Polytechnic University, China

Y. Q. Ni
The Hong Kong Polytechnic University, China

H.L.W. Chan
The Hong Kong Polytechnic University

Abstract

Smart magnetorheological (MR) dampers with embedded piezoelectric transducers have been developed to provide a closed-loop vibration control of bridge cables. The smart MR damper consists of a lead zirconate titanate (PZT) piezoelectric sensor integrated with a conventional MR damping device. The piezoelectric sensor is used to sense the external excitation forces exerted on the smart damper. The sensing-while-damping function of the smart damper offers great potential for real-time cable vibration control. To optimize the performance of the smart damper, the force sensors have been fabricated using different preloading conditions. The optimal condition has been determined from the calibration of the force sensors which was performed using force-controlled tests on a Material Test System (MTS). The performance tests of the smart MR damper have been conducted by mounting the smart MR damper on a MTS operating in a displacement-controlled excitation of sine waves with different driving conditions to the smart damper. The relationship between the applied current to the smart damper and the force sensed by the piezoelectric sensor is significant to provide the closed-loop vibration control. The experimental results proved that the smart MR damper has potential in the applications of real-time, closed-loop vibration control of civil and mechanical structures.

INTRODUCTION

Non-destructive detection and evaluation of mechanical and civil structures is highly desirable from the view point of safe and economic operation of installed structures. In order to minimize the effects of extreme loadings such as strong wind and heavy rain, the states of health in the structures are continuously monitored and activated when necessary. The structures will be equipped with an integrated monitoring system that can detect structural deterioration and damage and provide early warnings of structural failure [1].

Magnetorheological (MR) dampers have been extensively used in vibration control of civil and mechanical structures. They are easy to install without affecting the appearance of the structures. The application areas include the vibration control of the stay cables in cable-stayed bridges [2-5], seismic protection of infrastructures [6, 7] and vibration damping of automobiles [8, 9]. MR dampers are one of the most common applications for MR fluids. The MR fluids in the MR dampers are a suspension of micrometer - sized magnetic particles in a carrier fluid, usually a type of oil. The fluids have the ability to reversibly change their rheological characteristics when subjected to a magnetic field. In a MR damper, the free-flowing, linear viscous MR fluid can be changed to a semi-solid with controllable yield stress in milliseconds when exposed to an applied magnetic field [10]. By inputting different electrical currents to the electromagnet of the MR damper, the magnetic field applied to the MR fluid can be controlled. Consequently, the yield stress of the material and hence the yield force and rheological damping can also be readily controlled in milliseconds. When applied for structural vibration control, MR dampers can serve as passive dampers in the case of small-amplitude vibration and be activated when large vibration is coming, thus greatly reducing the power requirement.

While possessing controllable yield force and rheological damping capability, the existing MR dampers are incapable of sensing structural vibrations or external forces for implementing real-time, closed-loop vibration controls; they are currently used in open-loop mode of operation instead, and their controllable capability cannot be fully utilized. Initial studies indicate that appropriately implemented semi-active control systems using MR damping devices perform significantly better than passive devices [7, 11, 12]. It was proved that MR dampers can provide variable damping even after installation by tuning the damper current input to an appropriate value for a desired mode [13]. The semi-active devices have the following advantages: (a) they require low power to achieve controllable performance; (b) they are fail-safe devices that still serve as passive dampers even when the corresponding control system fails; (c) they can be easily integrated with or designed as structural components to form intelligent systems.

In order to fully utilize the capabilities of the MR dampers, suitable control strategies should be implemented practically. Since MR dampers are highly nonlinear, it is not easy to build an accurate inverse dynamic model for closed-loop operations of MR dampers. A force feedback control loop [14] is an alternative way to overcome the deficiency of implementing inverse dynamic modeling via an installation of force Feedback control by using force sensors (between the vibrating structures and the dampers) and MR dampers would be an effective method for mitigating structural vibration [14]. During the operation, the vibration mode signals will be captured by the sensors and then sent to the control system. The damper would readjust itself to the necessary damping after receiving the signal from the control. Therefore, it is highly desirable to develop and optimize smart MR dampers with embedded force sensors for providing real-time, force feedback control in a simple, cost-effective and reliable manner.

The most widely used force sensing materials are piezoelectric materials because of their wide usable frequency range, fast response and reliability [15]. They can exhibit a mechanical deformation when subjected to an electric field, or conversely, develop an electric field when subjected to pressure. The latter effect has been extensively utilized for force sensor application [16-18]. By integrating an appropriate piezoelectric sensor into the traditional MR damper, an external force exerted on the damper can be monitored. With the data of external force, a current can be calculated via a model to control the magnetic field and hence the resulting yield force and rheological damping of the damper in response to a variance in the external excitation. In this paper, several smart MR dampers with an embedded piezoceramic sensor have been fabricated using different preloading conditions. They were characterized using a Material Test System (MTS) 810 and the pre-stress of the piezoelectric sensor was optimized. The practical viability of the smart damper for structural vibration control is shown and discussed.

CONSTRUCTION OF THE SMART MR DAMPER

Figure 1 shows a schematic diagram and a photograph of a conventional damper [19]. The MR fluid is kept inside a cylindrical housing with a bearing and seal unit. The bearing and seal unit guides the movement of the piston and prevents the leakage of the MR fluid. By applying the current to the electromagnet through a pair of electrical wires, the MR fluid would be reversibly changed from a free-flowing, linear viscous fluid to a semi-solid with controllable yield stress such that the yield force and rheological damping of the damper can be changed accordingly.

To fabricate the smart MR damper with a self-sensing function, a piezoelectric force sensor was fabricated. A solid model of the piezoelectric force sensor is shown in Figure 2. The sensor consists of insulating wafers, a piezoelectric ceramic wafer, and two metal wafer electrodes mounted on either side of the piezoelectric wafer. In this study, a Ferroperm Pz28 PZT piezoceramic ring, having an outer diameter of 38 mm, an inner diameter of 13 mm and a thickness of 2 mm, was used as the piezoceramic wafer in the smart MR damper. Fired-on silver was used as the electrode and the wafer was poled across its thickness direction. Electrical wires were soldered to the metal wafer electrodes to deliver electrical charges generated from the piezoelectric wafer through a signal conditioning unit and a data acquisition unit. Insulating wafers were mounted between the metal wafer electrodes for electrical isolation. All these sensor components were stacked centrally under a mechanical pressure by using a threaded shaft protruding from an adaptor to a shaft hole opened in the connection support. The threaded shaft was insulated using a plastic band from the wafer electrodes and piezoelectric wafer.

Since it is not practical to use a piezoelectric material under tension, the technique of preloading should be performed on the piezoelectric force sensor. The force sensor is mechanically preloaded so that the tension forces can be measured and the piezoelectric element remains in compression during operation. An ideal preload would be infinitely elastic with only small mechanical force shunt. The preloading force should be high enough so that the piezoelectric wafer remains in compression during operation. The optimal level of preload depends on the

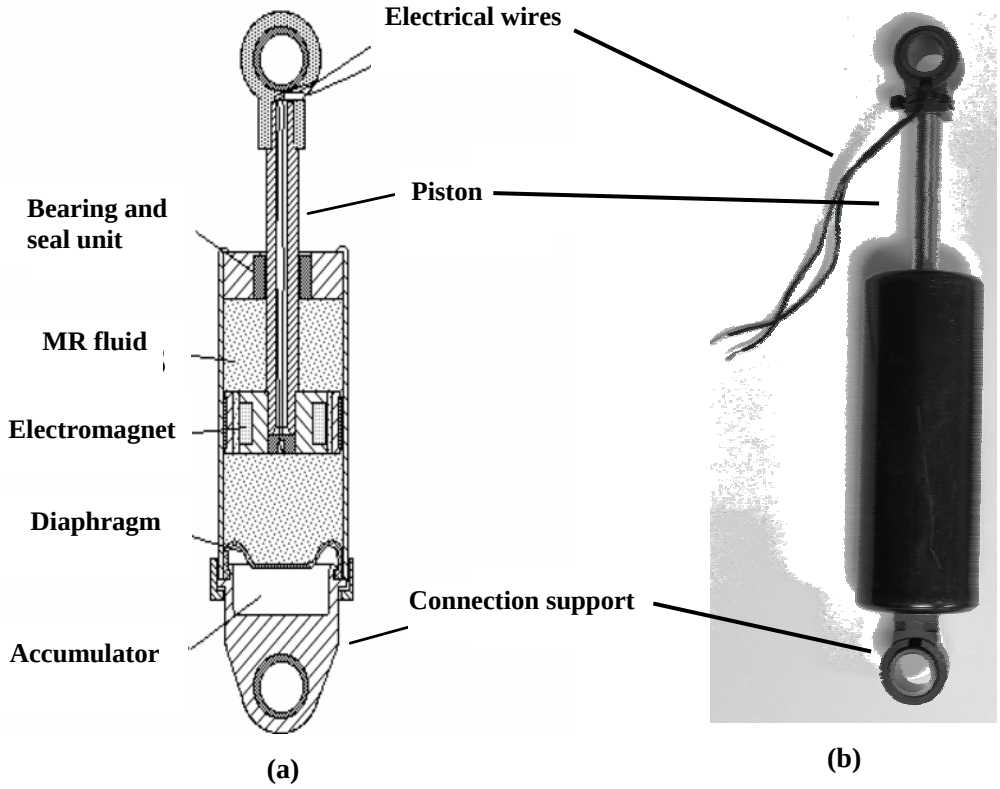

Figure 1. (a) A schematic diagram and (b) a photograph of a conventional damper.

magnitude of the load to be measured and pressure capacity of the piezoelectric wafer. To optimize the preloading, the force sensors were preloaded with torques of 20 Nm, 30 Nm and 40 Nm using a torque driver (Britool). In this study, a load cell (Tokyo Sokki Kenkyujo KC30MA) was used to calibrate the compression force exerted by the torque driver. The compression forces and stresses of the corresponding torques applied on the force sensor are shown in Table 1. During the preloading, the positive and negative electrodes should be connected to form a short-circuit condition to avoid accumulation of charges on the surfaces of the piezoelectric wafer. The torque was applied slowly to the threaded shaft until the torque driver was overloaded.

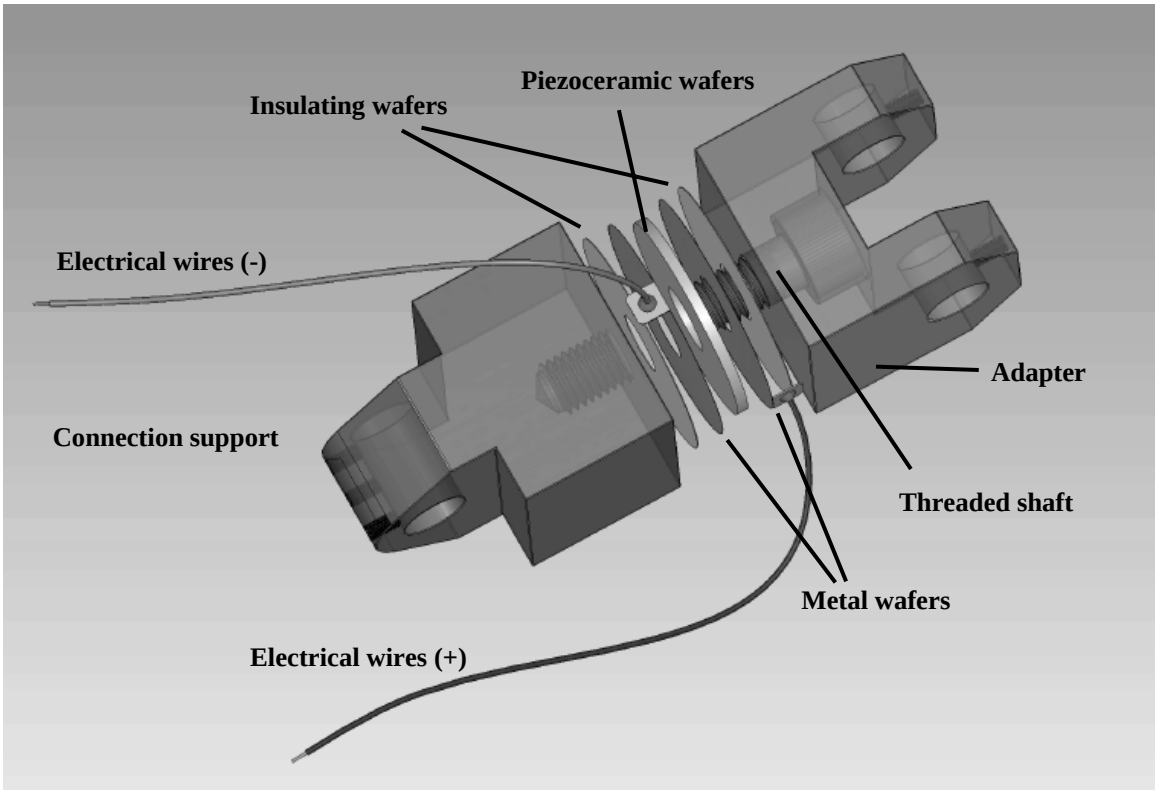

Figure 2. A solid model of a piezoelectric force sensor.

The smart MR damper with embedded piezoelectric force sensor was finally fabricated as shown in Figure 3. The smart damper includes the conventional MR damper with the attachment of the piezoelectric sensor for measuring the external forces exerted on the damper due to structural vibrations. Once the piezoelectric sensor senses the variances in the external forces exerted on the damper, the electrical signals would be generated in accordance with the variances in the pressures imposed onto their electroded surfaces. These signals can be used to assist for determining the current inputs to the electromagnet in order to control the magnetic field applied to the MR damper and hence the resulting yield force and rheological damping of the damper. Since the piezoelectric sensor is capable of monitoring real-time variances in the external forces, real-time control of the yield force and rheological damping of the damper according to the control strategies can be achieved.

Table 1: The relationship between the torque exerted by the torque driver and compression stress applied on the sensor.

Torque (N.m)	Compression stress (MPa)	Compression force (kN)
20	12	12
30	18	18
40	20	20

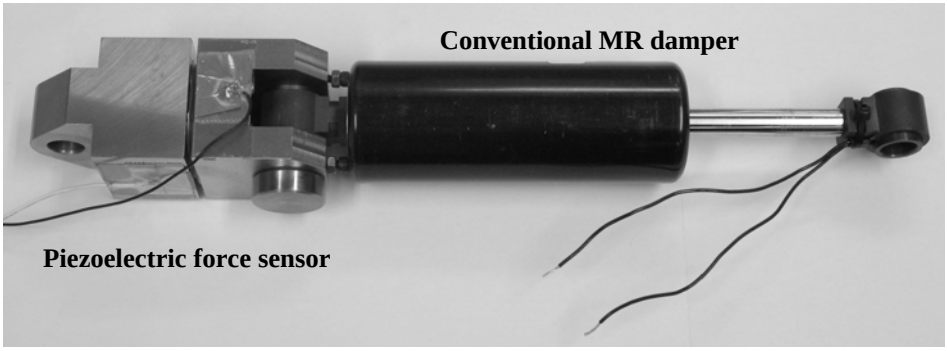

Figure 3. A photograph of a smart MR damper.

CHARACTERIZATION OF THE SMART MR DAMPER

The calibration of the piezoelectric sensor and performance tests on the smart MR dampers were carried out using a Material Test System (MTS) 810 as shown in Figure 4. For the convenience of mounting the smart damper onto the MTS for characterization, two connection adapters were fabricated and installed onto both ends of the smart MR damper. During the measurements, force-controlled and displacement-controlled tests were carried out using sine wave with the desired frequency and the desired force amplitude. The output charge signal of the piezoelectric force sensor was converted to voltage through a charge meter (Kistler 5015) and then recorded by a data acquisition system (National Instruments 635E). The displacement and force exerted to the damper / sensor by the MTS were also recorded in the MTS and the data acquisition system for further data analysis. At the same time, the preliminary signal patterns including the output voltage, force and displacement were recorded using a personal computer and displayed on a monitor. In practical, this enables a real-time control of the yield force and rheological damping can also be achieved by using the previous results to control the current inputs to the electromagnet of the MR damper afterwards.

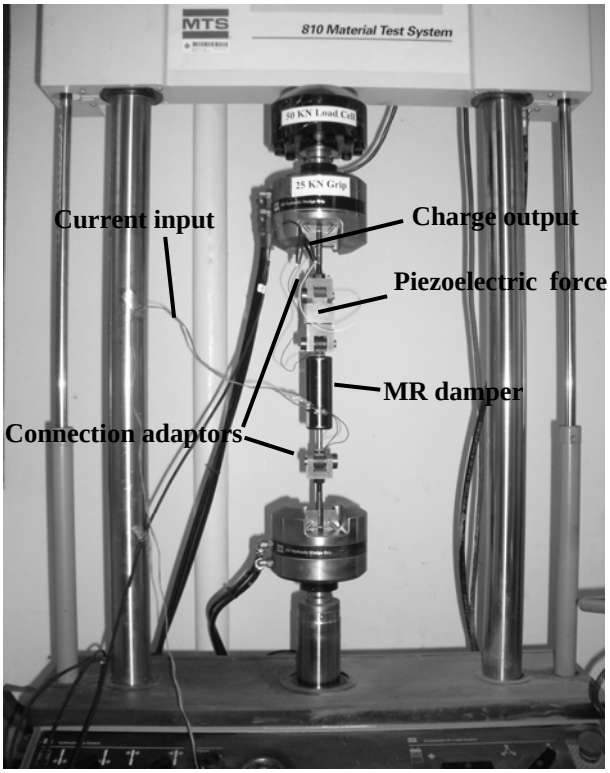

Figure 4. Experimental setup of calibration and performance tests of the smart MR damper.

Calibration of a Piezoelectric Force Sensor

For calibrating the piezoelectric force sensor, only the sensor was mounted on the MTS. The force-controlled tests were carried out using a sine wave with the frequency of 0.2 Hz, 1.0 Hz, 2.5 Hz, and 5.0 Hz and the force amplitude of 500 N, 1000 N, 1500 N and 2000 N. From the signals of sensor outputs and MTS driving forces, a sensitivity coefficient (force / voltage) can be obtained for each case of the tests. In Figure 5, the cases of sine wave excitations at a frequency of 1 Hz with different force amplitudes are shown. The time history of the sensor signals and MTS signals shows that the sensor signal, *V*, follows very well with the MTS force signal, *F*. A sensitivity coefficient *k* of the force sensor can be obtained from the slope of the line shown in the plots of force versus voltage as shown in the right column of plots in Figure 5 by minimizing the index of *J*:

$$k = \sum_{i=1}^{n} (F_i V_i) \Big/ \sum_{i=1}^{n} V_i^2 \tag{1}$$

$$J = \sum_{i=1}^{n} (F_i - kV_i)^2 \tag{2}$$

where *i* indicates sampling sequence and *n* is the total number of the data used for the calibration. To quantify the magnitude of the residual, the standard deviation is defined as:

$$\delta_{(F,kV)} = \sqrt{\frac{1}{n-1} \sum_{i=1}^{n} (F_i - kV_i)^2} \tag{3}$$

The values of *k* and $\delta_{(F, kQ)}$ of the piezoelectric force sensor with the preloading of 20 Nm, 30 Nm and 40 Nm are shown in Table 2, 3 and 4, respectively. It can be seen that the data is reliable with very small standard deviation in each case. Because of the dipole switching mechanism of the piezoelectric materials, the values of *k* increase when the excitation frequency decreases. The mean value of sensitivity coefficient, $\bar{k}$, is defined as:

$$\bar{k} = \frac{1}{N} \sum_{j=1}^{N} k_j \tag{4}$$

with the standard deviation given by:

$$\delta_{(k,\bar{k})} = \sqrt{\frac{1}{N} \sum_{j=1}^{N} (k_j - \bar{k})^2} \tag{5}$$

where *j* indicates the sequence of calibration cases and *N* is the total number of the calibration cases. The mean values of sensitivity of the force sensor under different preloading torques are summarized in Table 5. Among the three preloading conditions, the sensor with the preloading of 30 Nm has the maximum sensitivity of 0.638 kN/V. It can be concluded that a torque of 30 Nm is the optimal preloading condition for the piezoelectric force sensor. This sensor was integrated with the conventional MR damper into the smart MR damper.

Table 2: Calibration of the force sensor with a preloading of 20 Nm under sine wave excitations.

Force (kN)	Frequency (Hz)							
	0.2		1.0		2.5		5.0	
	k (kN/V)	$\delta_{(F, kV)}$ (%)	*k* (kN/V)	$\delta_{(F, kV)}$ (%)	*k* (kN/V)	$\delta_{(F, kV)}$ (%)	*k* (kN/V)	$\delta_{(F, kV)}$ (%)
0.5	-0.7292	2.569	-0.5891	1.919	-0.5858	1.042	-0.5890	1.004
1.0	-0.7279	2.624	-0.5852	2.278	-0.5844	1.523	-0.5860	1.522
1.5	-0.7197	2.849	-0.5819	2.429	-0.5817	1.814	-0.5825	1.998
2.0	-0.7197	2.848	-0.5781	2.665	-0.5780	1.911	-0.5791	2.225

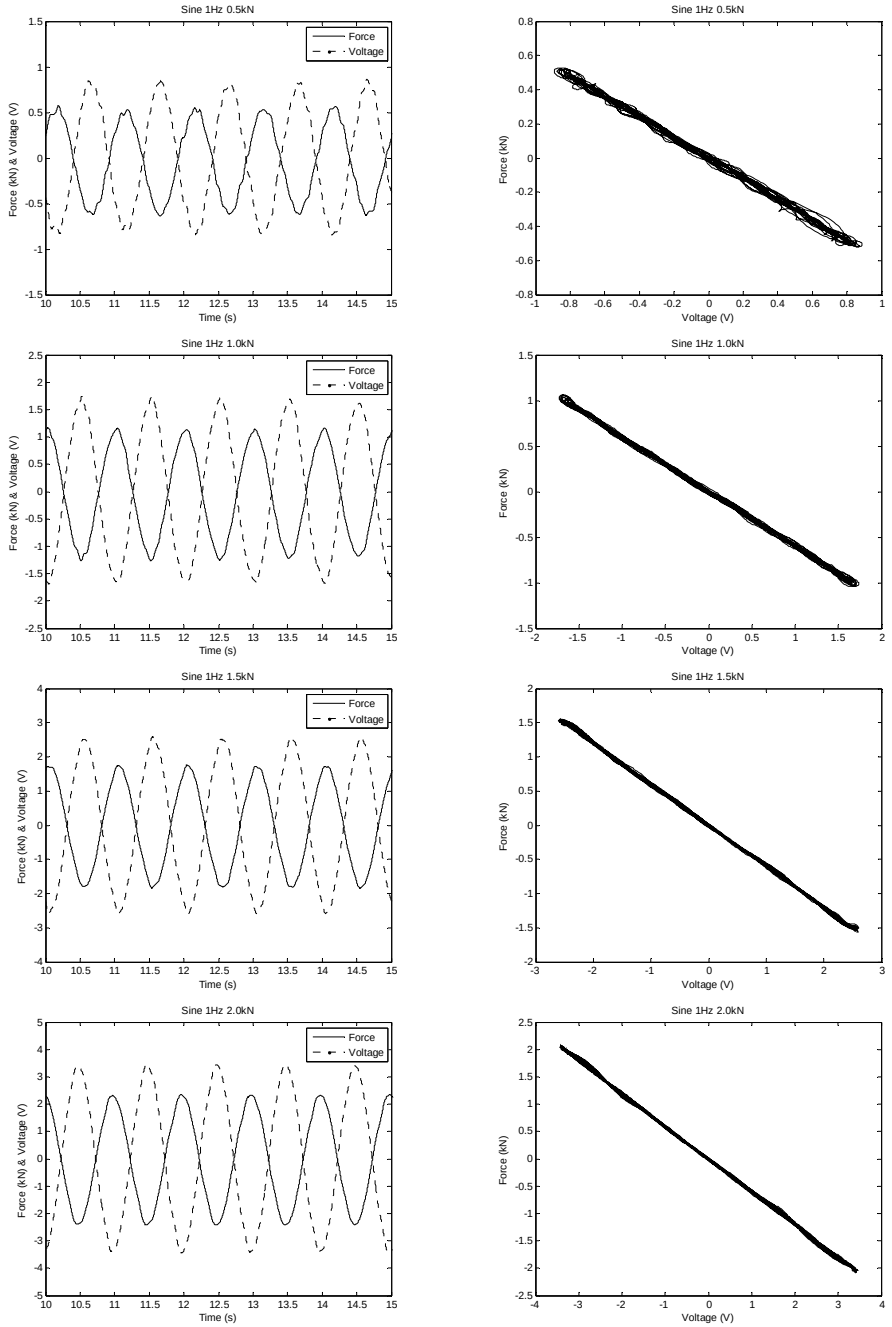

Figure 5. Calibration of the piezoelectric force sensor under a force-controlled excitation.

Table 3: Calibration of the force sensor with a preloading of 30 Nm under sine wave excitations.

Force (kN)	Frequency (Hz)							
	0.2		1.0		2.5		5.0	
	k (kN/V)	$\delta_{(F,kV)}$ (%)	k (kN/V)	$\delta_{(F,kV)}$ (%)	k (kN/V)	$\delta_{(F,kV)}$ (%)	k (kN/V)	$\delta_{(F,kV)}$ (%)
0.5	-0.7518	1.517	-0.6013	1.873	-0.5988	0.839	-0.5995	0.913
1.0	-0.7535	2.088	-0.6021	2.031	-0.5990	1.068	-0.5997	1.550
1.5	-0.7515	2.682	-0.6017	2.368	-0.5984	1.586	-0.5992	2.425
2.0	-0.7496	2.844	-0.6006	2.798	-0.5975	2.217	-0.5984	2.958

Table 4: Calibration of the force sensor with a preloading of 40 Nm under sine wave excitations.

Force (kN)	Frequency (Hz)							
	0.2		1.0		2.5		5.0	
	k (kN/V)	$\delta_{(F, kV)}$ (%)	k (kN/V)	$\delta_{(F, kV)}$ (%)	k (kN/V)	$\delta_{(F, kV)}$ (%)	k (kN/V)	$\delta_{(F, kV)}$ (%)
0.5	-0.7004	1.979	-0.5691	1.677	-0.5667	0.872	-0.5689	1.142
1.0	-0.7016	1.876	-0.5673	1.851	-0.5659	1.356	-0.5599	1.712
1.5	-0.7016	2.308	-0.5645	2.435	-0.5635	1.874	-0.5597	2.257
2.0	-0.7005	2.753	-0.5629	2.842	-0.5618	2.601	-0.5637	2.645

Table 5: Summary of the mean sensitivity and the standard deviation of the force sensor with different preloading conditions.

	Torque (Nm)		
	20	30	40
$\bar{k}$ (kN/V)	-0.6186	-0.6380	-0.5986
$\delta_{(k, \bar{k})}$ (%)	6.11	6.59	10.15

Performance Tests of a Smart MR Damper

Displacement-controlled tests on the smart MR damper with an embedded piezoelectric sensor were conducted to investigate the agreement between the signals obtained from the senor and MTS and to investigate the damping characteristic of the damper. During the measurement, the force exerted onto the smart damper can be expressed as

$$F\ (\mathrm{N}) = k\ (\mathrm{N/V}) \times V\ (\mathrm{V}) \qquad (6)$$

The comparison between the force signals obtained from the force sensor according to Equation (6) and from the MTS is shown in Figure 6. The displacement excitation was a sine wave with a displacement amplitude of 5 mm and a frequency of 5 Hz and the current input to the damper is 0 A, 0.25 A, 0.50 A, 0.75 A and 1.00 A, respectively. Good agreement was found between the force signals obtained from the sensor and the MTS except the case with the applied current of 0 A. Relative root mean squares for force signals from MTS (F) and PZT sensor ($\bar{k}\ V$) is

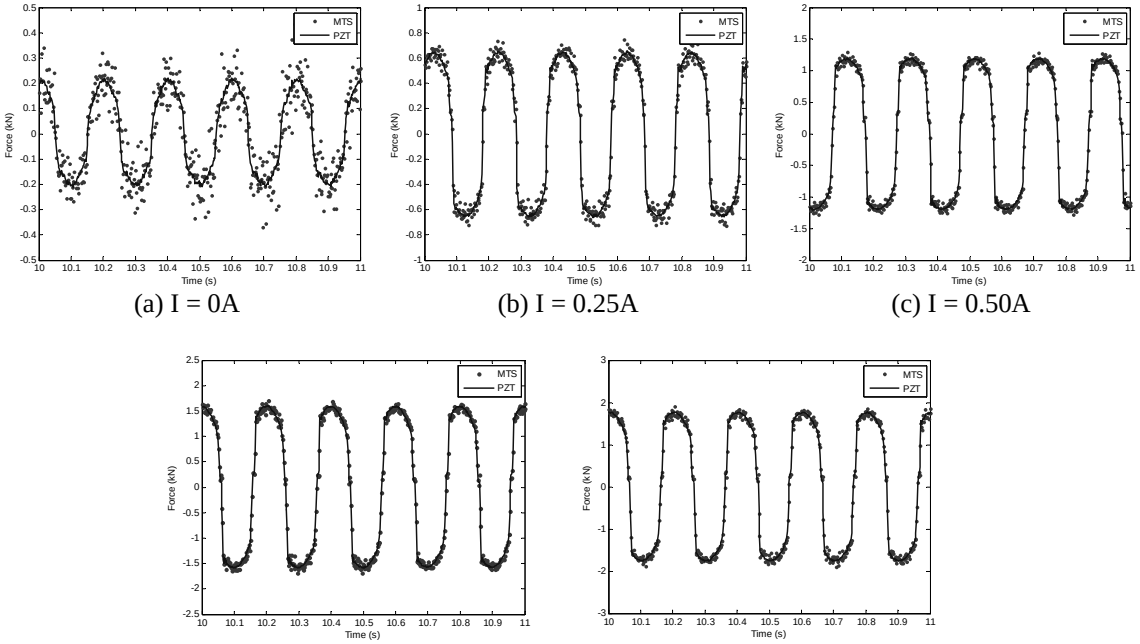

(a) I = 0A (b) I = 0.25A (c) I = 0.50A

(d) I = 0.75A (e) I = 1.00A

Figure 6. Comparison between the force signals obtained from the sensor and the MTS.

defined as:

$$\delta_{(F,\bar{k}V)} = \sqrt{\frac{1}{n}\sum_{i=1}^{n}(F_i - \bar{k}V_i)^2} \Big/ \sqrt{\frac{1}{n}\sum_{i=1}^{n}F_i^2} \tag{7}$$

where *i* indicates sampling sequence and *n* is the total number of the data used for the calculation. It is found that the values are reasonably small except the case with the applied current of 0 A as shown in Table 6. The relatively big difference may be due to the difference between the resolution of the embedded sensor for MTS and the magnitude of the damper force. Therefore, the signal from the piezoelectric sensor predicted well the damper force. The force-displacement and force-velocity hysteresis loops of the smart MR damper are shown in Figure 7(a) and 7(b), respectively. The results were derived from the piezoelectric force senor and the displacement transducer of MTS. It is shown that the magnitude of the damper force increases with the applied current.

Table 6: Summary of the mean sensitivity and the standard deviation of the force sensor with different preloading conditions.

Current (A)	0	0.25	0.50	0.75	1.00
$\delta_{(F,\ \bar{k}\ V)}$ (%)	32.27	9.97	5.53	4.76	4.54

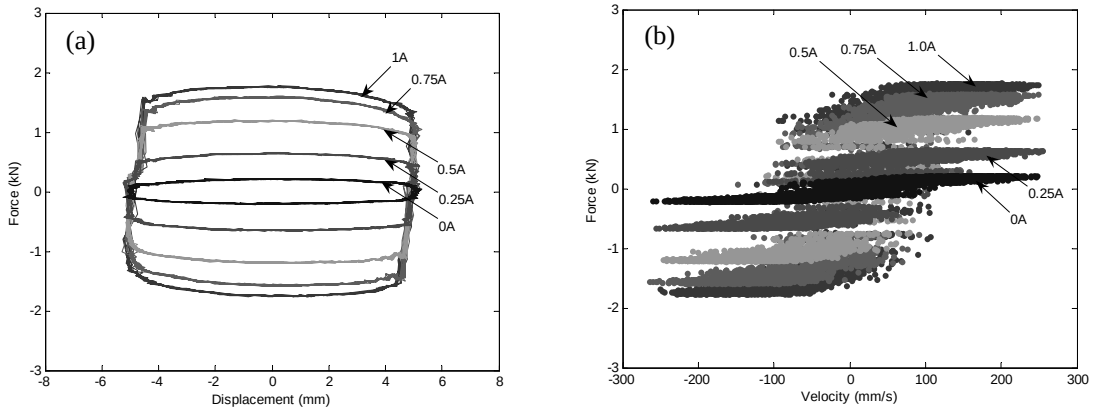

Figure 7. (a) force-displacement curve and (b) force-velocity hysteresis loops of the smart MR damper.

CONCLUSIONS

A smart MR damper possessing an attractive functionality of force sensing-while-damping with a high degree of sensor-damper collocation was fabricated and characterized. The calibration of the piezoelectric force sensors was carried out by force-controlled tests under sine wave excitations of different frequencies. A mean sensitivity coefficient was obtained with small standard deviation. It is found that the preloading torque of 30 Nm is the optimal condition for fabricating the developed sensor. The smart MR damper with the embedded piezoelectric sensor was characterized using displacement-controlled tests with different applied current to the MR damper. Good agreement was found between force signals from the force sensor and from the MTS. Therefore, the smart MR damper with the embedded piezoelectric force sensor has good potential in the applications of real-time, closed-loop vibration control of civil and mechanical structures.

ACKNOWLEDGEMENTS

This work was supported by The Hong Kong Polytechnic University under Central Research Grant through an inter-faculty collaborative research project (G-YD85) between Department of Applied Physics and Department of Civil and Structural Engineering, which is gratefully acknowledged.

REFERENCES

1. Teng, J.G., Ko, J.M., Chan, H.T.H., Ni, Y.Q., Xu, Y.L., Chan, S.L., Chau, K.T. and Yin, J.H., 'Third-generation Structures: Intelligent High-performance Structures for Sustainable Urban Systems,, Proceedings of International Symposium on Diagnosis, Treatment & Regeneration for Sustainable Urban Systems, Ibaraki, Japan, 2003, 41-55.
2. Ni, Y.Q., Chen, Y., Ko, J.M. and Cao, D.Q., 'Neuro-control of Cable Vibration Using Semi-active Magneto-rheological Dampers', Engineering Structures, 24 (2002) 295-307.
3. Ni, Y.Q., Duan, Y.F., Chen, Z.Q. and Ko, J.M., 'Damping Identification of MR-damped Bridge Cables from In-situ Monitoring under Wind-rain-excited Conditions', In: Liu, S.-C. (ed.), Smart Structures and Materials 2002: Smart Systems for Bridges, Structures, and Highways, SPIE, Bellingham, 4696(2002) 41-51.
4. Ko, J.M., Duan, Y.F. and Ni, Y.Q., 'Modeling of a Full-Scale MR Damper and Its Application in Open-Loop Vibration Control of Stay Cables', In: Tomizuka, M. (ed.), Smart Structures and Materials 2005: Sensors and Smart Structures Technologies for Civil, Mechanical, and Aerospace Systems, SPIE, Bellingham, 5765(2005) 690-700.
5. Duan, Y.F., Ni, Y.Q. and Ko, J.M., 'Cable Vibration Control Using Magnetorheological Dampers," Journal of Intelligent Material Systems and Structures', 17(4)(2006) 321-325.
6. Spencer, B.F., Jr., Carlson, J.D., Sain, M.K. and Yang, G., 'On the Current Status of Magnetorheological Dampers: Seismic Protection of Full-scale Structures', In: Proceedings of American Control Conference, New Mexico, USA, 1997, 458-462.
7. Dyke, S.J., Spencer, B.F., Jr., Sain, M.K. and Carlson, J.D., 'An Experimental Study of MR Dampers for Seismic Protection', Smart Materials and Structures, 7(5)(1998) 693-703.
8. Choi, S.B., Nam, M.H. and Lee, B.K., 'Vibration Control of a MR Seat Damper for Commercial Vehicles', Journal of Intelligent Material systems and Structures, 11(2000) 936–944.
9. Peck, Kevin L., 'Magneto-Rheological Shock Absorber for an off-road motorcycle', California Polytechnic State University, San Luis Obispo, BS Thesis, 2001.
10. Carlson, J.D. and Weiss, K.D., 'A Growing Attraction to Magnetic Fluids', Machine Design, 66(1994) 61-66.
11. Johnson, E.A., Christenson, R.E. and Spencer, B.F., Jr., 'Semiactive damping of cables with sag', Computer-Aided Civil and Infrastructure Engineering, 18(2003) 132-146.
12. Duan, Y.F., Ni, Y.Q. and Ko, J.M., 'State-Derivative Feedback Control of Cable Vibration Using Semiactive Magnetorheological Dampers', Computer-Aided Civil and Infrastructure Engineering, 20(6)(2005) 431-449.
13. Ni, Y.Q., Chen, Y., Ko, J.M. and Zheng, G., 'Optimal voltage/current input to ER/MR dampers for multi-switch control of stay cable vibration', *Proceedings of the Third World conference on Structural Control*, F. Casciati (ed), Chichester, 3(2003), 767-775.
14. Christenson, R.E. 'Semiactive Control of Civil Structures for Natural Hazard Mitigation: Analytical and Experimental Studies', PhD Dissertation, Department of Civil Engineering and Geological Sciences, University of Notre Dame, 2003.
15. Yamamoto, T., 'Ferroelectric properties of the $PbZrO_3$-$PbTiO_3$ system', Jpn. J. Appl. Phys. 35 (1996) 5104-5108.
16. Or, S.W., Chan, H.L.W. and Liu P.C.K., 'Development of Smart Transducer with Embedded Sensor for Automatic Process Control of Ultrasonic Wire Bonding', Smart Structures and Systems, 1(1)(2005) 47-61.
17. Shen, Y.T., Winder, E., Xi, N., Pomeroy, C.A. and Wejinya, U.C., 'Closed-loop optimal control-enabled piezoelectric microforce sensors', IEEE-ASME Transactions on Mechatronics, 11(4)(2006) 420-427.
18. Smith, S.T. and Seugling, R.M., 'Sensor and actuator considerations for precision, small machines', Journal of the International Societies for Precision Engineering and Nanotechnology, 30(3)(2006) 245-264.
19. Snyder, R.A., Kamath, G.M. and Wereley, N.M., 'Characterization and Analysis of Magnetorheological Damper Behavior under Sinusoidal Loading', *AIAA Journal* 39(7)(2001) 1240-1253.